

THERMOELECTRIC PROPERTIES INVESTIGATION OF Ni/Co DOPED ZrCoBi HALF-HEUSLER ALLOY[†]

 Mahmoud Al-Elaimi*

Department of Basic Sciences, Preparatory Year Deanship, University of Ha'il, Ha'il, Saudi Arabia

**E-mail: m.alelaimi@gmail.com*

Received March 26, 2023; revised March 30, 2023; accepted March 31, 2023

Half-Heusler (HH) thermoelectric (TE) composites have been intensively inspected due to their excellent TE properties in the medium-to high-temperature range. First-principle calculations make it easier to discover or improve more HH compounds. This article presents an ab initio theoretical evaluation of TE properties of ZrCoBi Half-Heusler alloy, when doped with Nickel (Ni), using FP-LAPW and the semi classic Boltzmann theory. Thermoelectric parameters were calculated using BoltzTraP code, like Seebeck coefficient (S), electrical conductivity to relaxation time ratio (σ/τ), electronic thermal conductivity to relaxation time ratio (κ_e/τ), thermoelectric power factor to relaxation time ratio ($S^2\sigma/\tau$), and the dimensionless figure-of-merit (ZT) in a temperature range of 0 – 500 K. Calculated Seebeck coefficient reveals that the studied alloys show a tendency to conduct as p-type with balanced TE performance between both charge carriers (holes and electrons). A high electronic thermal conductivity value is found, which predicts a potential use in heat sink applications for the investigated alloys. Obtained results, such as a high thermoelectric power factor and $ZT \cong 1$, postulate that ZrCo_{1-x}Ni_xBi alloys could have potential thermoelectric applications.

Key words: *ab initio calculations; Half-Heusler alloys; ZrCoBi; Ni/Co doping; Thermoelectric properties; Transport properties*

PACS: 72.80.Tm, 72.15.Jf, 74.25.Fy, 85.80.Fi, 73.50.Lw

INTRODUCTION

Since humans have started depending on fossil fuel energy, many environmental issues appeared. Climate change and global warming are of the most serious problems humans have to face. Recently, a decline rate of environmental issues was noticed due to COVID-19 breakout. However, these issues began to increase gradually after recovering from this pandemic [1]. Developing new renewable and sustainable energy technologies has become a vital choice for mankind in 21st century to confront such threats. Finding new and reliable metamaterials with desired thermoelectric (TE) characteristics has attracted more ambitious researchers and manufacturers as well. The new metamaterials with enhanced properties are utilized in many practical applications.

Generally, the performance of TE metamaterials is estimated by the thermoelectric figure-of-merit (ZT) that is described by the following formula:

$$ZT = \frac{\sigma S^2}{\kappa} T$$

here S, σ , σS^2 , κ , T are Seebeck coefficient, electrical conductivity, thermoelectric power factor, thermal conductivity and absolute temperature, respectively [2-4].

The thermal conductivity (κ) has electronic and lattice contributions:

$$\kappa = \kappa_e + \kappa_l$$

Where κ_e is the electronic thermal conductivity and κ_l is the lattice thermal conductivity. The ZT of a TE metamaterial can be enhanced by increasing the σS^2 and/or by decreasing κ . But the close interdependent relations among S, σ , and κ_e via the carrier concentration leads to a real challenge in optimizing the TE transport properties while κ_l is considered relatively independent [5].

Generally, in order to produce promising TE metamaterials, a high ZT must be achieved [6-8], which can be fulfilled by optimizing σS^2 through tuning the carrier concentration. Usually, tuning carrier concentration can be obtained either by doping or by band engineering [9, 10], and reducing the thermal conductivity κ [11-13].

Among all TE materials, Half-Heusler (HH) compounds are excellent candidates for TE applications, such as spintronics [14], thermoelectric [15], optoelectronic [16], piezoelectric [17], shape memory alloys [18], and solar cell applications [19]. HH compounds have been intensively investigating since their discovery in 1903 by Friedrich Heusler [20] for their promising characteristics, such as thermoelectricity [15], high thermoelectric power factor σS^2 [21], tunable band gap [22], magnetism [23], durable mechanical properties [24], semi-metallicity [25], notable thermal stabilities [26], etc. HH compounds typically exhibit a valence electron count (VEC) of 18 per unit cell and have cubic MgAgAs structure (F43m). They are ternary intermetallic with a general formula of XYZ, where X is usually the d-electron transition metal, Y is a f-electron transition metal and Z is a p-electron element [27].

However, the main issue with HH compounds is their relatively high thermal conductivity that reduces ZT value and, accordingly, limits their TE performance. For that reason, many researchers have recently spent many efforts in

[†] Cite as: M. Al-Elaimi, East Eur. J. Phys. 2, 234 (2023), <https://doi.org/10.26565/2312-4334-2023-2-26>

© M. Al-Elaimi, 2023

searching for enhanced HH thermoelectric materials. That enhancement can be attained through reducing the lattice thermal conductivity via optimizing nanoparticle phonon scattering centers [28], point defects [29], and grain size reduction [30].

Since experimental improving the TE materials is sometimes time consuming and/or costs a lot, many researchers prefer ab initio calculations. This procedure allows screening bigger sets of compounds along with shorter time using efficient codes and modern computers [31]. Hence, new high performance TE compounds might be identified. For example, Qureshi, M.T. et al. studied the Cu₂O based semiconductor materials and observed an elevation in the Seebeck coefficient consequent of Ag doping. They stated that these materials are promising candidates for modern electric devices. [32]. Huang et al. found interstitial Sn atoms in substitution leads to increase S and decrease the κ_e of n-type NbCoSb; thus, an enhanced figure-of-merit of ~ 0.56 is acquired [33]. Nenuwe et al. announced figure-of-merit values of ($ZT = 3.27$ and 1.43), suggesting that FeCrSb, and RuCrSb are potential materials for TE applications [34]. Dhakshayani et al. found that XCaB ($X = \text{Na, K and Rb}$) compounds have desired ferromagnetic and half-metallic behaviors with ZT of 1.00, and can be used for TE and spintronics applications [35].

One of the recently studied HH compounds with interesting TE properties is ZrCoBi. Nura Ibrahim et al. studied the TE properties of the heavily doped ZrCoBi. The results revealed desired TE properties, such as a high σS^2 at high-temperature region, and a high ZT of ~ 0.35 for ZrCo_{0.75}Ni_{0.25}Bi at 900 K [36]. Zhu et al. announced the discovery the Half-Heusler of ZrCoBi with a huge TE conversion efficiency of $\sim 9\%$, which is computed at a wide temperature variation of about 500 K, and reached a good ZT amount of about 1.42 at 973 K [37]. Yazdani-Kachoei, M. et al. studied the electronic and structural characteristics of ZrRhBi and ZrCoBi. They showed that those compounds have high Seebeck value and low electrical conductivity [38]. Hangtian Zhu et al. have studied the TE characteristics of ZrCoBi-based Half-Heuslers. They showed that those compounds can be used as mid- and high-temperature TE power generators [39].

In this research, the ab-initio calculations are used to investigate the TE properties of Ni-doped Half-Heusler ZrCoBi compounds. In the following section, the computational details are briefly summarized. The effects of Ni doping into Co site on the thermoelectric behavior of ZrCoBi were demonstrated and discussed in section 3. The conclusion is given in section 4.

COMPUTATIONAL DETAILS

Half-Heusler ZrCo_{1-x}Ni_xBi compounds have a cubic lattice structure with space group of $F\bar{4}3m$. The Ni concentrations (x) are chosen to be (0, 0.25, 0.75 and 1) such that an optimal structural stability is achieved. Their structural, thermal, and electronic properties were discussed in details in a previous study [40]. Where the Full-Potential Wien2k package [41], the Linearized Augmented Plane Wave (FP-LAPW) method [42], the generalized gradient approximation (PBE-GGA) [43] were used. The convergence test limits of the self-consistent calculations were chosen to be 0.1×10^{-3} Ry for the determined total energy and 0.1×10^{-3} e for crystal charge. In this work, the thermoelectric transport coefficients were calculated using BoltzTraP code, which is interfaced within Wien2k. The calculations are based on DFT and Boltzmann theory [44].

RESULTS AND DISCUSSION

In this section, the thermoelectric behavior of Ni-doped ZrCoBi alloys are presented and discussed. Seebeck coefficient (S), electrical conductivity to relaxation time ratio (σ/τ), electronic thermal conductivity to relaxation time ratio (κ_e/τ) were calculated in the temperature range 0 – 500 K. Then the thermoelectric power factor to relaxation time ratio ($S^2\sigma/\tau$), and the dimensionless figure-of-merit (ZT) were worked out. The temperature (T) dependence of the Seebeck coefficient (S) is plotted in Fig. 1, where S behavior for both charge carriers is illustrated. It is noticed that Seebeck coefficient reaches its optimal value in the low-temperature region then decreases exponentially with increase in temperature.

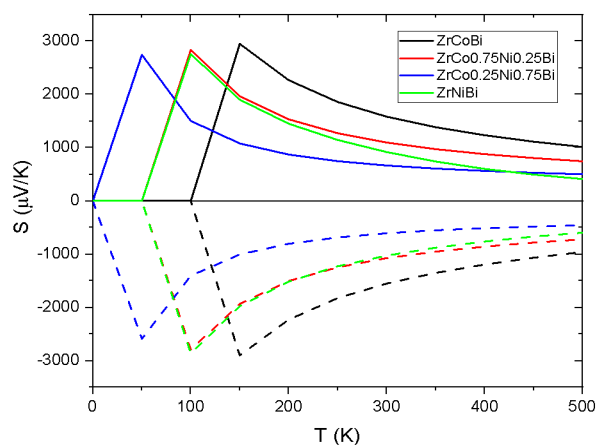


Figure 1. Temperature dependence of Seebeck coefficient of ZrCo_{1-x}Ni_xBi. Solid (dashed) lines denote hole (electron) charge carriers.

The S_{max} values for hole (electron) charge carrier are found to be $2.95 \times 10^3 \mu\text{V/K}$ at 150 K ($-2.90 \times 10^3 \mu\text{V/K}$ at 150 K) for ZrCoBi, $2.83 \times 10^3 \mu\text{V/K}$ at 100 K ($-2.79 \times 10^3 \mu\text{V/K}$ at 100 K) for ZrCo_{0.75}Ni_{0.25}Bi, $2.74 \times 10^3 \mu\text{V/K}$ at 50 K ($-2.59 \times 10^3 \mu\text{V/K}$ at 50 K) for ZrCo_{0.25}Ni_{0.75}Bi, and $2.76 \times 10^3 \mu\text{V/K}$ at 100 K ($-2.86 \times 10^3 \mu\text{V/K}$ at 100 K) for ZrNiBi. Ni substitution in Co site shifts the S curves to a lower temperature region, especially the ZrCo_{0.25}Ni_{0.75}Bi. A rapprochement of S_{max} values for both hole and electron charge carrier is noticed for all doping cases. From these values, it is expected that ZrCo_{1-x}Ni_xBi can split between both charge carriers (holes and electrons) quasi-Fermi levels at donor/acceptor interface.

The dependence of Seebeck coefficient on charge carrier concentration (n) of ZrCo_{1-x}Ni_xBi alloys are plotted in Fig. 2. The S_{max} values relative to n are located at 0, 1, 1, and 3 for ZrCoBi, ZrNiBi, ZrCo_{0.75}Ni_{0.25}Bi, and ZrCo_{0.25}Ni_{0.75}Bi, respectively. It is obviously noticed that the change of temperature does not influence S values for both charge carriers. However, Ni-doping shifts the curves to the higher positive (hole) concentration region, especially the ZrCo_{0.25}Ni_{0.75}Bi. According to the obtained S_{max} and n values, it is found that ZrCo_{1-x}Ni_xBi can alter between both charge carriers (holes and electrons) with the same thermoelectric efficiency and work as p-type alloys.

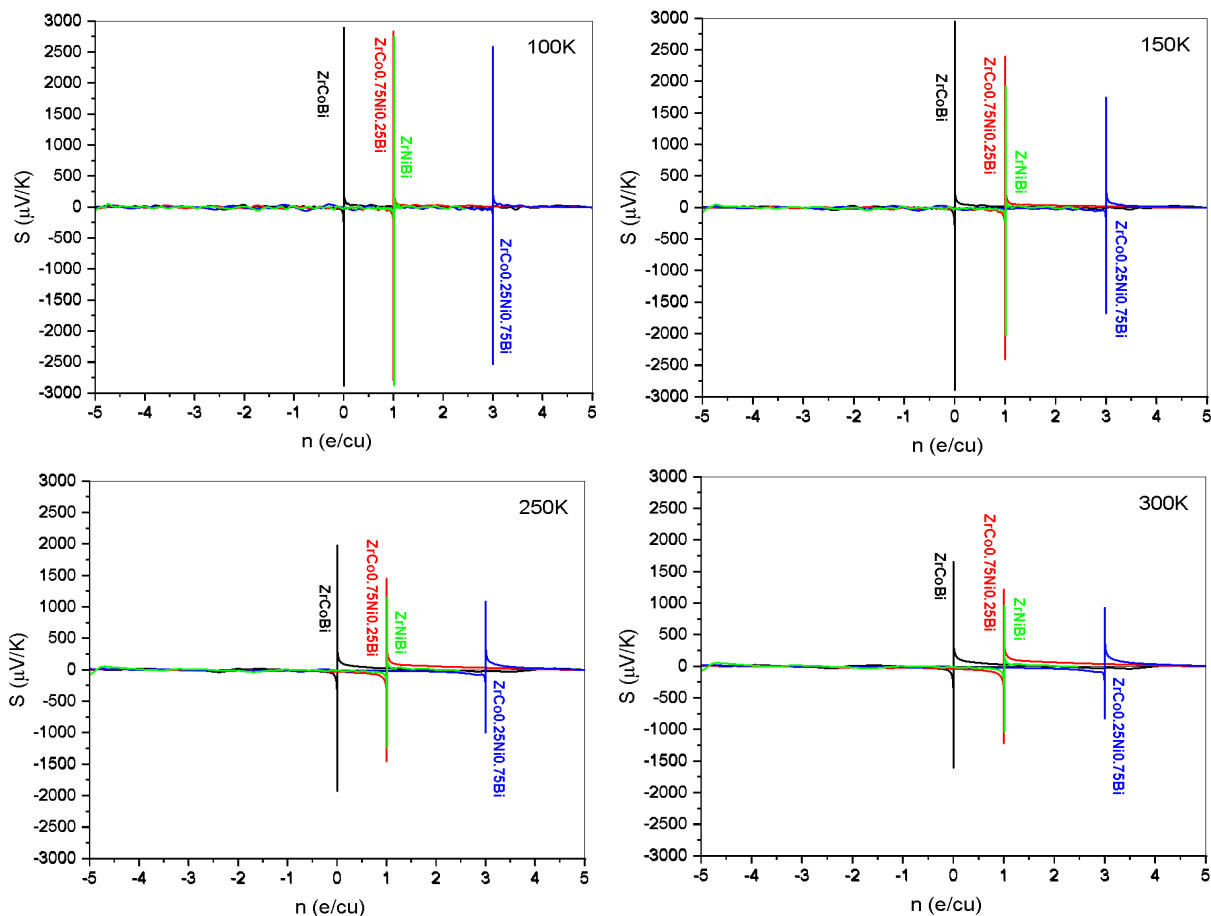


Figure 2. The charge carrier concentration dependence of Seebeck coefficient of ZrCo_{1-x}Ni_xBi at 100, 150, 250, and 300 K.

The potential applicability of ZrCo_{1-x}Ni_xBi as a thermoelectric material not only depends on the thermoelectric power, but also on the most important charge transport properties, namely the electrical and thermal conductivities. The temperature dependence of electrical conductivity to relaxation time ratio (σ/τ) is calculated. σ/τ is found directly (inversely) proportional to T (S) satisfying the Mott formula [45]. A remarkable preference of ZrCo_{0.25}Ni_{0.75}Bi is noticed, as shown in Fig. 3.

The desired response of σ/τ implies a growing of n that elevates holes to the conduction band. The highest σ/τ value is found to be for ZrCo_{0.25}Ni_{0.75}Bi for all chosen temperatures. By comparison to the other studied compounds, the elevated σ/τ amount of ZrCo_{0.25}Ni_{0.75}Bi for both charge carrier concentrations exhibits significantly large band dispersion at the band edges, and hence a small effective mass. Moreover, the computed σ/τ values are found nearly the same for both charge carriers, which is in agreement with the previous conclusion about the ability of all Ni-doped compounds to exchange between charge carriers (holes and electrons).

Fig. 4 illustrates that σ/τ is directly proportional to n at 300 K. The computed $(\sigma/\tau)_{max}$ amounts of the p-type (n-type) doping regime are $3.06 \times 10^{20} (\Omega\text{ms})^{-1}$ at $1.76 \text{ e(c.u.)}^{-1}$ ($3.81 \times 10^{20} (\Omega\text{ms})^{-1}$ at $-3.49 \text{ e(c.u.)}^{-1}$) for ZrCoBi, $1.71 \times 10^{20} (\Omega\text{ms})^{-1}$ at $4.90 \text{ e(c.u.)}^{-1}$ ($2.30 \times 10^{20} (\Omega\text{ms})^{-1}$ at $-3.34 \text{ e(c.u.)}^{-1}$) for ZrCo_{0.75}Ni_{0.25}Bi,

$1.06 \times 10^{20} (\Omega\text{ms})^{-1}$ at 5.53 e(c.u)^{-1} ($2.79 \times 10^{20} (\Omega\text{ms})^{-1}$ at $-2.88 \text{ e(c.u)}^{-1}$) for $\text{ZrCo}_{0.25}\text{Ni}_{0.75}\text{Bi}$, and $2.52 \times 10^{20} (\Omega\text{ms})^{-1}$ at 2.46 e(c.u)^{-1} ($4.16 \times 10^{20} (\Omega\text{ms})^{-1}$ at $-2.47 \text{ e(c.u)}^{-1}$) for ZrNiBi . A preference of σ/τ is clearly noticed for n-type doping regime over p-type at 300 K.

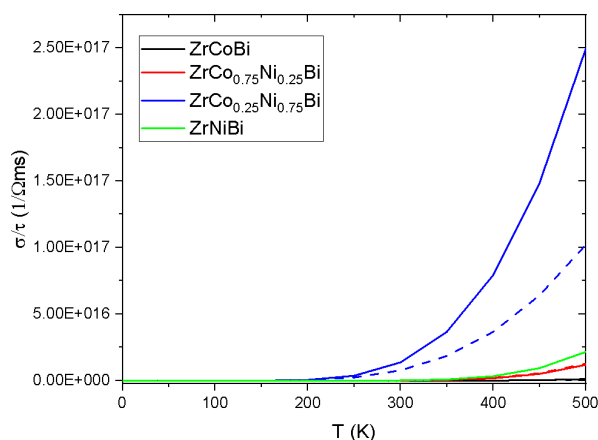


Figure 3. The temperature dependence of electrical conductivity to relaxation time ratio (σ/τ) of $\text{ZrCo}_{1-x}\text{Ni}_x\text{Bi}$. Solid (dashed) lines denote hole (electron) charge carriers

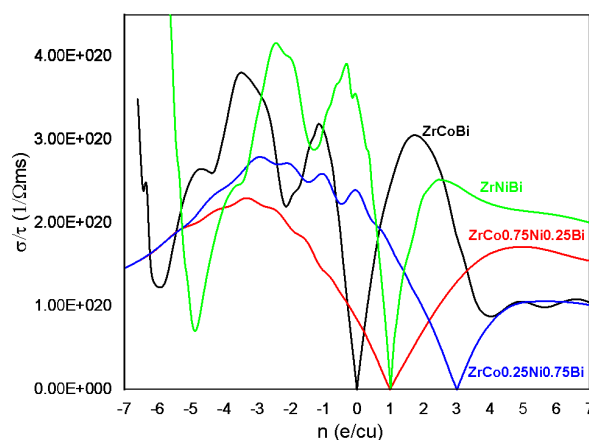


Figure 4. The charge carrier concentration dependence of electrical conductivity to relaxation time ratio (σ/τ) of $\text{ZrCo}_{1-x}\text{Ni}_x\text{Bi}$ at 300 K

The variation of the electronic thermal conductivity to relaxation time ratio (κ_e/τ) with temperature is demonstrated in Fig. 5. It is found that κ_e/τ vs T and σ/τ vs T curves have a comparable behavior. They are directly (inversely) proportional to T (S) that satisfies the Mott formula. Below room temperature, there is a monotonic variation in κ_e/τ . While, beyond room temperature, the κ_e/τ shows strong temperature dependence. This implies a stoichiometric composition of the alloys, and an increasing charge carrier flow with the raising temperature. In addition, Wiedemann–Franz law, which describes the κ_e and σ relationship, is also verified as κ_e/σ is found to be constant. The high electronic thermal conductivity values, especially for $\text{ZrCo}_{0.25}\text{Ni}_{0.75}\text{Bi}$, suggests a use in heat sink applications for studied compounds.

Besides S , the thermoelectric power factor to relaxation time ratio ($S^2\sigma/\tau$) is an excellent measure that grants credibility to $\text{ZrCo}_{1-x}\text{Ni}_x\text{Bi}$ to be used in thermoelectric applications. Fig. 6 presents the temperature dependence of the thermoelectric power factor to relaxation time ratio for both charge carriers. It is found that $S^2\sigma/\tau$ raises as the temperature elevates for both doping systems. A clear preference of $\text{ZrCo}_{0.25}\text{Ni}_{0.75}\text{Bi}$ is noticed, which exhibits a sharp elevation above ambient temperature region. This behavior indicates that $\text{ZrCo}_{0.25}\text{Ni}_{0.75}\text{Bi}$ has promising thermoelectric properties, like waste heat usage in power generators.

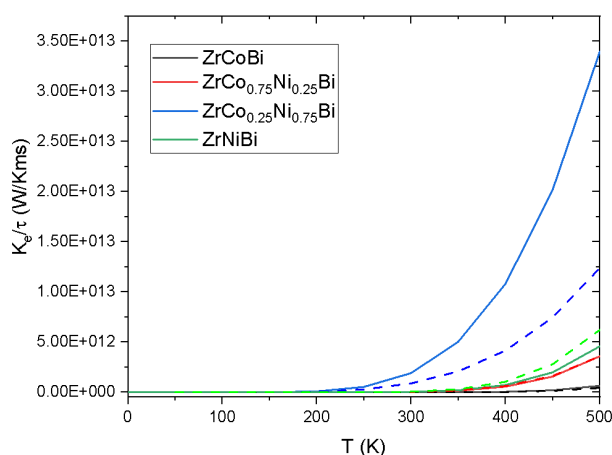


Figure 5. The temperature dependence of the electronic thermal conductivity to relaxation time ratio (κ_e/τ) of $\text{ZrCo}_{1-x}\text{Ni}_x\text{Bi}$. Solid (dashed) lines denote hole (electron) charge carriers

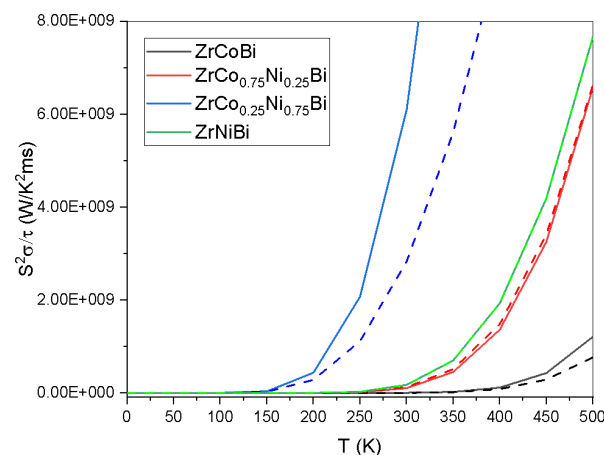


Figure 6. The temperature dependence of the thermoelectric power factor to relaxation time ratio ($S^2\sigma/\tau$) of $\text{ZrCo}_{1-x}\text{Ni}_x\text{Bi}$. Solid (dashed) lines denote hole (electron) charge carriers

Fig. 7 demonstrates the charge carrier concentration dependence of $S^2\sigma/\tau$ at 300 K. The evaluated maximum $S^2\sigma/\tau$ values at 300K are found 6.33×10^{11} , 3.23×10^{11} , 3.90×10^{11} , and $6.87 \times 10^{11} \text{ W/K}^2\text{ms}$ for ZrCoBi , $\text{ZrCo}_{0.75}\text{Ni}_{0.25}\text{Bi}$, $\text{ZrCo}_{0.25}\text{Ni}_{0.75}\text{Bi}$, and ZrNiBi , respectively. The elevated $S^2\sigma/\tau$ values foresee that $\text{ZrCo}_{1-x}\text{Ni}_x\text{Bi}$ are good future candidates for thermoelectric device applications.

The results of electrical conductivity, electronic thermal conductivity, and Seebeck coefficient were used to calculate the figure-of-merit (ZT). The variation of the ZT with temperature corresponding to the hole and electron charge carrier of the present alloys are shown in Fig. 8. The obtained ZT values are nearly equal to 1 for all compounds up to 150K. At higher temperatures, ZT drops marginally, but remain in the high ZT region for all compounds except ZrNiBi. ZrNiBi shows a strong temperature dependence as its ZT value drops more promptly in the high temperature region. Being ZT is equal to 1 up to 150K and about 0.90 till 500K predicts beneficial thermoelectric properties of $\text{ZrCo}_{1-x}\text{Ni}_x\text{Bi}$ alloys. Experimental values of figure-of-merit for Ni-doped ZrCoBi are not available for comparison.

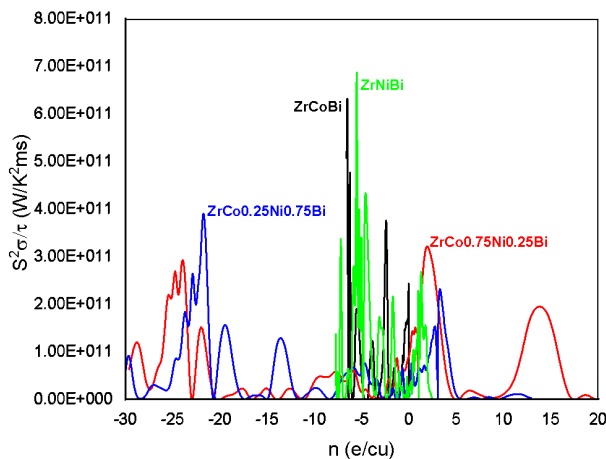


Figure 7. The charge carrier concentration dependence of thermoelectric power factor to relaxation time ratio ($S^2\sigma/\tau$) of $\text{ZrCo}_{1-x}\text{Ni}_x\text{Bi}$ at 300 K

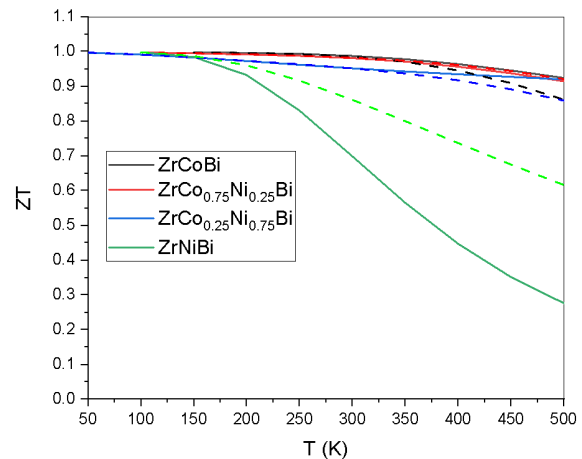


Figure 8. Figure-of-merit (ZT) of $\text{ZrCo}_{1-x}\text{Ni}_x\text{Bi}$. Solid (dashed) lines denote hole (electron) charge carriers

Based on Seebeck coefficient, electrical conductivity, electronic thermal conductivity, thermoelectric power factor, and relatively high ZT value, $\text{ZrCo}_{1-x}\text{Ni}_x\text{Bi}$ are predicted to be good TE materials. These compounds might be used in TE applications, such as thermoelectric power generator from waste heat and sustainable energy systems. Moreover, the current findings may inspire experimentalists to explore these compounds at wider doping concentration and temperature ranges.

CONCLUSION

In this paper, the transport parameters of the cubic ternary $\text{ZrCo}_{1-x}\text{Ni}_x\text{Bi}$ half-Heusler alloys have been computed using FP-LAPW and Boltzmann theory. The transport parameters, calculated by using BoltzTraP code, are Seebeck coefficient (S), electrical conductivity to relaxation time ratio (σ/τ), electronic thermal conductivity to relaxation time ratio (κ_e/τ), thermoelectric power factor to relaxation time ratio ($S^2\sigma/\tau$), and the dimensionless figure-of-merit (ZT) in the temperature range 0 – 500 K. Findings show that $\text{ZrCo}_{1-x}\text{Ni}_x\text{Bi}$ have a p-type doping character with ability to alter between hole and electron charge carrier. The high value of S at low temperature range proposes favorable thermoelectric applications of the studied compounds. A remarkable high σ/τ value of $\text{ZrCo}_{0.25}\text{Ni}_{0.75}\text{Bi}$ is noticed. The high electronic thermal conductivity value especially for $\text{ZrCo}_{0.25}\text{Ni}_{0.75}\text{Bi}$ suggests that these compounds can be used in the heat sink applications. Due to the high values of thermoelectric power factor and figure-of-merit ($ZT \cong 1$), potential thermoelectric device applications are predicted, such as sustainable energy systems.

Acknowledgement

Author is thankful to Prof. Dr. A. A. Mubarak (Physics department, college of science and arts - Rabigh, King Abdulaziz university) for fruitful discussions and suggestions.

ORCID ID

©Mahmoud Al-Elaimi, <https://orcid.org/0000-0001-6985-1012>

REFERENCES

- [1] M.M. Alam, M.A. Aktar, N.D.M. Idris, and A.Q. Al-Amin, *J World Development Sustainability*, **2**, 100048 (2023), <https://doi.org/10.1016/j.wds.2023.100048>
- [2] C. Gayner, and K. K. Kar, *J. Progress in Materials Science*, **83**, 330-382 (2016), <https://doi.org/10.1016/j.pmatsci.2016.07.002>
- [3] R. Liu, H. Chen, K. Zhao, Y. Qin, B. Jiang, T. Zhang, G. Sha, X. Shi, C. Uher and W. Zhang, *J. Advanced Materials*, **29**(38), 1702712 (2017), <https://doi.org/10.1002/adma.201702712>
- [4] T. Zhu, C. Fu, H. Xie, Y. Liu and X. Zhao, *Advanced Energy Materials*, **5**(19), 1500588 (2015), <https://doi.org/10.1002/aenm.201500588>
- [5] A. Mubarak, S. Saad, F. Hamioud and M. Al-Elaimi, *J. Solid State Sciences*, **111**, 106397 (2021), <https://doi.org/10.1016/j.solidstatesciences.2020.106397>
- [6] J. Wei, L. Yang, Z. Ma, P. Song, M. Zhang, J. Ma, F. Yang and X. Wang, *J. Journal of Materials Science*, **55**, 12642-12704 (2020), <https://doi.org/10.1007/s10853-020-04949-0>

- [7] D. Li, Y. Gong, Y. Chen, J. Lin, Q. Khan, Y. Zhang, Y. Li, H. Zhang and H. Xie, *J. Nano-Micro Letters*, **12**, 1-40 (2020), <https://doi.org/10.1007/s40820-020-0374-x>
- [8] P.A. Finn, C. Asker, K. Wan, E. Bilotti, O. Fenwick, and C.B. Nielsen, *J. Frontiers in Electronic Materials*, **1**, 677845 (2021), <https://doi.org/10.3389/femat.2021.677845>
- [9] Y. Zheng, T.J. Slade, L. Hu, X.Y. Tan, Y. Luo, Z.-Z. Luo, J. Xu, Q. Yan and M. G. Kanatzidis, *J. Chemical Society Reviews*, **50** (16), 9022-9054 (2021), <https://doi.org/10.1039/D1CS00347J>
- [10] A. Kumar, S. Bano, B. Govind, A. Bhardwaj, K. Bhatt and D. Misra, *J. of Electronic Materials* **50**, 6037-6059 (2021), <https://doi.org/10.1007/s11664-021-09153-7>
- [11] Z. Bu, W. Li, J. Li, X. Zhang, J. Mao, Y. Chen, and Y. Pei, *J. Materials Today Physics*, **9**, 100096 (2019), <https://doi.org/10.1016/j.mtphys.2019.100096>
- [12] S. Roychowdhury, R.K. Biswas, M. Dutta, S.K. Pati, and K. Biswas, *J. ACS Energy Letters*, **4** (7), 1658-1662 (2019), <https://doi.org/10.1021/acseenergylett.9b01093>
- [13] S. Li, J. Yang, J. Xin, Q. Jiang, Z. Zhou, H. Hu, B. Sun, A. Basit, and X. Li, *J. ACS Applied Energy Materials*, **2** (3), 1997-2003 (2019), <https://doi.org/10.1021/acsaem.8b02096>
- [14] K. Elphick, W. Frost, M. Samiepour, T. Kubota, K. Takanashi, H. Sukegawa, S. Mitani and A. Hirohata, *J. Science technology of advanced materials*, **22** (1), 235-271 (2021), <https://doi.org/10.1080/14686996.2020.1812364>
- [15] K. Xia, C. Hu, C. Fu, X. Zhao and T. Zhu, *J. Applied Physics Letters*, **118** (14), 140503 (2021), <https://doi.org/10.1063/5.0043552>
- [16] F. Parvin, M. Hossain, I. Ahmed, K. Akter, and A. Islam, *J. Results in Physics*, **23**, 104068 (2021), <https://doi.org/10.1016/j.rinp.2021.104068>
- [17] Z. Almaghbash, O. Arbouche, A. Dahani, A. Cherifi, M. Belabbas, A. Zenati, H. Mebarki, and A. Hussain, *J. International Journal of Thermophysics*, **42**, 1-19 (2021), <https://doi.org/10.1007/s10765-020-02755-z>
- [18] S. Dhanal, A. Ghaste, V. Akkimardi, S. Kori, and C. Bhosale, *AIP Conference Proceedings*, **2162**(1), 020002 (2019), <https://doi.org/10.1063/1.5130212>
- [19] V.K. Solet, S. Sk, and S.K. Pandey, *J. Physica Scripta*, **97**(10), 105711 (2022), <https://doi.org/10.1088/1402-4896/ac93c1>
- [20] T. Graf, C. Felser and S.S. Parkin, *J. Progress in solid state chemistry*, **39**(1), 1-50 (2011), <https://doi.org/10.1016/j.progsolidstchem.2011.02.001>
- [21] G.A. Naydenov, P.J. Hasnip, V. Lazarov, and M. Probert, *J. Journal of physics: Materials*, **2**(3), 035002 (2019), <https://doi.org/10.1088/2515-7639/ab16fb>
- [22] M.K. Bamgbose, *J. Applied Physics A*, **126**(564), 1-8 (2020), <https://doi.org/10.1007/s00339-020-03691-3>
- [23] D. Vishali, and R. John, *J. Journal of Crystal Growth*, **583**, 126556 (2022), <https://doi.org/10.1016/j.jcrysgro.2022.126556>
- [24] W.Y.S. Lim, D. Zhang, S.S.F. Duran, X.Y. Tan, C.K.I. Tan, J. Xu, and A. Suwardi, *J. Frontiers in Materials*, **8**, 745698 (2021), <https://doi.org/10.3389/fmats.2021.745698>
- [25] R. Majumder, M.M. Hossain, and D. Shen, *J. Modern Physics Letters B*, **33**(30), 1950378 (2019), <https://doi.org/10.1142/S0217984919503780>
- [26] E. Rausch, B. Balke, S. Ouardi and C. Felser, *J. Energy Technology*, **3** (12), 1217-1224 (2015), <https://doi.org/10.1002/ente.201500183>
- [27] A.S. Gzyl, A.O. Oliynyk, and A. Mar, *J. Crystal Growth Design*, **20**(10), 6469-6477 (2020), <https://doi.org/10.1021/acs.cgd.0c00646>
- [28] M. Sato, Y.W. Chai, and Y. Kimura, *ACS Appl. Mater. Interfaces*, **13**(21), 25503-25512 (2021), <https://doi.org/10.1021/acsaami.1c03525>
- [29] T. Chibueze, A. Raji, and C. Okoye, *J. Phys. Chem. Solids*, **139**, 109328 (2020), <https://doi.org/10.1016/j.jpcs.2019.109328>
- [30] X. Zhang, S. Li, B. Zou, P. Xu, Y. Song, B. Xu, Y. Wang, G. Tang, and S. Yang, *J. of Alloys and Compounds*, **901**, 163686 (2022), <https://doi.org/10.1016/j.jallcom.2022.163686>
- [31] A. Mubarak, S. Tariq, F. Hamioud, and B. Alsobhi, *Journal of Physics: Condensed Matter*, **31**(50), 505705 (2019), <https://doi.org/10.1088/1361-648X/ab3140>
- [32] M.T. Qureshi, F. Ullah, R.S.A. Hameed, M. Al-Elimi, J. Humadi, A. Nassar, M. Badr, K.A. Halim, and M. Saleem, *J. Ceramics International*, (2023), <https://doi.org/10.1016/j.ceramint.2023.03.103>
- [33] L. Huang, Q. Zhang, Y. Wang, R. He, J. Shuai, J. Zhang, C. Wang, and Z. Ren, *J. Physical Chemistry Chemical Physics*, **19**(37), 25683-25690 (2017), <https://doi.org/10.1039/C7CP04801G>
- [34] N. Nenuwe, and E. Omugbe, *J. Current Applied Physics*, **49**, 70-77 (2023), <https://doi.org/10.1016/j.cap.2023.02.013>
- [35] Y. Dhakshayani, G. Suganya, and G. Kalpana, *Journal of Crystal Growth*, **583**, 126550 (2022), <https://doi.org/10.1016/j.jcrysgro.2022.126550>
- [36] N. Ibrahim, R.A. Ahmed, H. Adri, and I. Reisy, *J. Materials Today Communications*, **32**, 103908 (2022), <https://doi.org/10.1016/j.mtcomm.2022.103908>
- [37] H. Zhu, R. He, J. Mao, Q. Zhu, C. Li, J. Sun, W. Ren, Y. Wang, Z. Liu and Z. Tang, *J. Nature communications*, **9**(1), 1-9 (2018), <https://doi.org/10.1038/s41467-018-04958-3>
- [38] M. Yazdani-Kachoei, and S. Jalali-Asadabadi, *Journal of alloys compounds*, **828**, 154287 (2020), <https://doi.org/10.1016/j.jallcom.2020.154287>
- [39] H. Zhu, J. Mao, Z. Feng, J. Sun, Q. Zhu, Z. Liu, D.J. Singh, Y. Wang, and Z. Ren, *J. Science advances*, **5**(6), eaav5813 (2019), <https://doi.org/10.1126/sciadv.aav5813>
- [40] M. Al-Elaimi, *East Eur. J. Phys.* (2), 103-111 (2022), <https://doi.org/10.26565/2312-4334-2022-2-13>
- [41] P. Blaha, K. Schwarz, P. Sorantin, and S. Trickey, *J. Computer physics communications*, **59**(2), 399-415 (1990), [https://doi.org/10.1016/0010-4655\(90\)90187-6](https://doi.org/10.1016/0010-4655(90)90187-6)
- [42] P. Hohenberg, and W. Kohn, *J. Physical Review*, **136**(3B), B864 (1964), <https://doi.org/10.1103/PhysRev.136.B864>
- [43] J.P. Perdew, K. Burke, and M. Ernzerhof, *J. Physical review letters*, **77**(18), 3865 (1996), <https://doi.org/10.1103/PhysRevLett.77.3865>
- [44] G.K. Madsen, and D.J. Singh, *J. Computer physics communications*, **175**(1), 67-71 (2006), <https://doi.org/10.1016/j.cpc.2006.03.007>
- [45] M. Cutler, and N. F. Mott, *J. Physical Review*, **181**(3), 1336 (1969), <https://doi.org/10.1103/PhysRev.181.1336>

**ДОСЛІДЖЕННЯ ТЕРМОЕЛЕКТРИЧНИХ ВЛАСТИВОСТЕЙ СПЛАВУ НАПІВГЕЙСЛЕРА $ZrCoBi$,
ЛЕГОВАНОГО Ni/Co
Махмуд Аль Елаймі**

Факультет фундаментальних наук, деканат підготовчого року, Університет Хаїль, Хаїль, Саудівська Аравія

Термоелектричні (ТЕ) композити Half-Heusler (НН) були перевірені через їхні відмінні ТЕ властивості в діапазоні середніх і високих температур. Розрахунки на основі першопринципів полегшують відкриття або покращення більшої кількості сполук НН. У статті представлено теоретичну оцінку ТЕ властивостей сплаву Half-Heusler $ZrCoBi$, легovanого нікелем (Ni), з використанням FP-LAPW і напівкласичної теорії Больцмана. Термоелектричні параметри розраховувалися за допомогою коду BoltzTraP, наприклад, коефіцієнт Зеебека (S), відношення електропровідності до часу релаксації (σ/τ), відношення електронної теплопровідності до часу релаксації (κ_e/τ), відношення коефіцієнта термоелектричної потужності до часу релаксації ($S^2\sigma/\tau$), а також безрозмірну добротність (ZT) в діапазоні температур 0-500 К. Розрахований коефіцієнт Зеебека показує, що досліджувані сплави демонструють тенденцію до провідності р-типу зі збалансованою ТЕ характеристикою між обома носіями заряду (дірки та електрони). Знайдено високе значення електронної теплопровідності, що передбачає потенційне використання досліджуваних сплавів у тепловідвідних програмах. Отримані результати, такі як високий коефіцієнт термоелектричної потужності та $ZT \cong 1$, припускають, що сплави $ZrCo_{1-x}Ni_xBi$ можуть мати потенційне термоелектричне застосування.

Ключові слова: *ab initio* розрахунки; сплави напівгейслера; $ZrCoBi$; легування Ni/Co ; термоелектричні властивості; транспортні властивості